

A Neural Network Based Compensation of Thermal Infrared Data Considering Environmental Temperature Variations

Seong Ho Song

Hallym University, Hallymdaehak-gil 1 Chunchon, Gangwon, Korea

Article Info

Volume 83

Page Number: 6758 - 6763

Publication Issue:

March - April 2020

Article History

Article Received: 24 July 2019

Revised: 12 September 2019

Accepted: 15 February 2020

Publication: 05 April 2020

Abstract:

In this paper, infrared data correction algorithm is suggested based on neural network functional approximation when the environmental temperatures such as air temperature are varying. To compensate infrared data, the relationship between infrared data and environmental temperatures is investigated first. Based on the relationship, a neural network approach is applied to identify a function which can be utilized to compensate the influence of environmental temperatures on infrared data. Through experiments the proposed neural network based algorithm is shown to reduce the influence of environmental temperatures on the infrared data effectively by comparing with polynomial based functional approximation approaches

Keywords: Thermal infrared Data, compensation algorithm, neural network, environmental temperature variation.

I. INTRODUCTION

Recently, infrared thermal imaging cameras are widely used for the screening of fertile infectious diseases. In order to detect accurate body temperatures, infrared cameras should be well calibrated. The difficulties of infrared camera calibration lie in the nonlinear characteristics of thermal detectors. A conventional way of data correction in infrared cameras is to use some target temperature source for compensation. As a target temperature source, thermal electric coolers or black body sources are often used. Using this source, a look-up table is established for compensation of infrared thermal data from infrared cameras. This kind of off-line correction process should be done first. Recently, on-line scene-based methods are widely studied in the literature. Even though this procedure is successfully done, additional calibrations should be proceeded considering environmental conditions because the sensitivity of infrared cameras is varying depending on detector temperatures and environmental ambient temperatures.

II. INFRARED CAMERA MODEL

In general, an infrared camera measurement model can be described by the following equation

$$y_{ij}(t) = a_{ij}(T_d, T_a, T_l, T_b)x_{ij}(t) + b_{ij}(T_d, T_a, T_l, T_b) \quad (1)$$

Where y_{ij}, x_{ij} are respectively infrared camera output and infrared detector input of (i,j)-th pixel. a_{ij}, b_{ij} are model coefficients and T_d, T_a, T_l, T_b are respectively camera ambient temperature, circuit amplifier temperature, lens temperature, and temperature of detector back plate. The infrared camera measurement model is usually given as a first-order input-output equation like (1). The model coefficients are depending on various environmental temperatures, so we should investigate the relationship between the coefficients and environmental temperature parameters. In order to clarify the relationship, we adopt Pearson coefficient to measure the correlation between thermal infrared data and these environmental parameters. Pearson coefficient is obtained by the following equation.

$$r = \frac{\sum XY - \frac{\sum X \sum Y}{N}}{\left\{ \sum X^2 - \frac{(\sum X)^2}{N} \right\} \left\{ \sum Y^2 - \frac{(\sum Y)^2}{N} \right\}} \quad (2)$$

In (2), N is the number of data and X, Y are respectively thermal infrared data and these environmental parameters. Here, thermal infrared data are

observed using blackbody whose temperature is set to a constant one. The Pearson coefficient is calculated using the experimental data with respect to each environmental parameters. The closer to 1 the Pearson coefficient for some environmental parameter is, the larger the correlation between the parameter and the thermal infrared data is. Table 1 represents the experimental results of Pearson coefficients for each environmental parameter. In the experiment, the temperature of target blackbody source has been changed from to 15°C to 35°C. As can be seen from Table 1, the camera ambient temperature is the most influential parameter on the camera model output. In general, an infrared camera measurement model for i-th row j-th column pixel element can be described by the following equation considering camera environmental temperature.

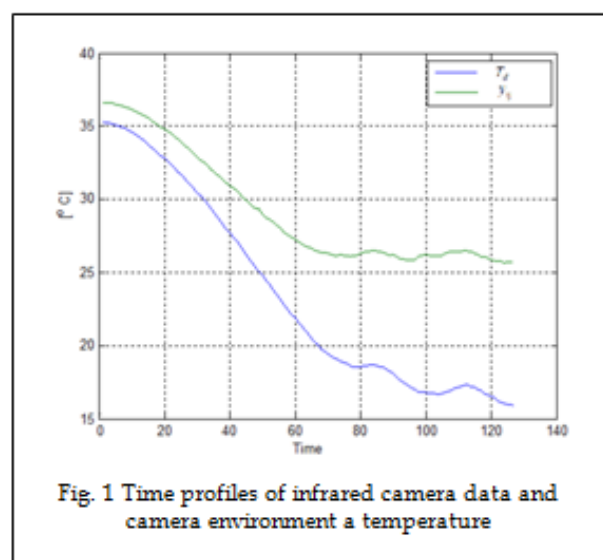
$$y_{ij}(t) = a_{ij}(T_0)x_{ij}(t) + b_{ij}(T_0) + f_{ij}(T_e) \quad (3)$$

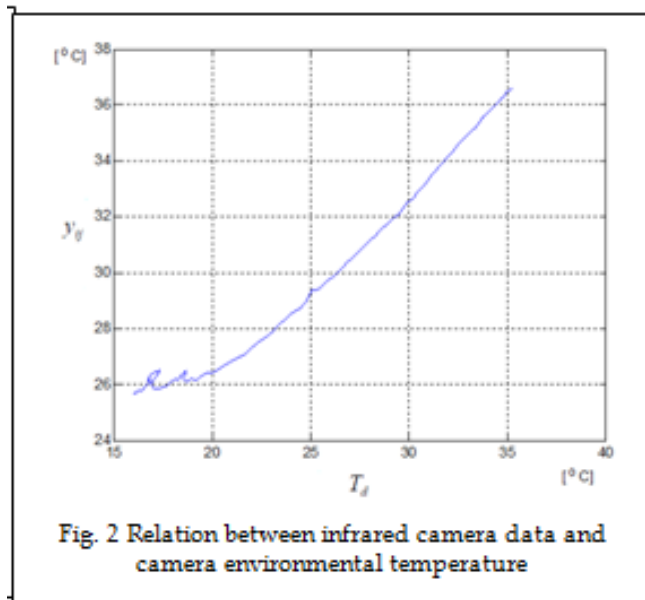
Table 1. Pearson coefficient

Blackbody Temperature	T_d	T_a	T_l	T_b
15°C	0.9982	0.2398	-0.9769	-0.8495
20°C	0.9970	0.4119	-0.8783	-0.6329
25°C	0.9976	0.0840	-0.4988	0.5821
30°C	0.9977	0.7390	-0.3567	0.7103
35°C	0.9985	0.7373	-0.8375	-0.3007

temperature sensor located in the infrared camera. As shown in the figure, the infrared camera outputs and camera environmental temperatures are considerably correlated. So, it can be easily figured out that the function $f_{ij}(T_e)$ in the model equation (1) is a function of the environmental temperature difference between the nominal camera environment temperatures T_0 and the real camera environmental temperature T_e , $\Delta T = T_e - T_0$. The functions f_{ij} can be defined as follows

where are respectively infrared camera temperature output and thermal input for (i,j)-th pixel element. The model nominal coefficients are model coefficients determined at nominal camera environment temperature and are the additional output function depending on camera environmental temperature. In order to obtain an accurate object temperature, the function should be estimated as much exactly as you can and compensated. Figure 1 represents the time profiles of the infrared camera output and camera environmental temperature when blackbody temperature is set to be 30°C. The experimental data were obtained when camera ambient temperature was varying from to 20°C to 50°C. Camera ambient temperatures are measured by the





$$f_{ij}(T_e) = f_{ij}(T_e - T_0) \quad (4)$$

Figure 2 shows the relationship between the infrared camera output and camera environmental temperatures. Usually it is chosen to be the room temperature $T_0 = 25^\circ C$. For example; the nominal coefficients a_{ij}, b_{ij} can be obtained using the equations (3) with $f_{ij}(T_e) = f_{ij}(T_e - T_0) = 0$ and (4) in Fig.2. So a compensation function \bar{f}_{ij} for a function f_{ij} is estimated and using that mapping, we can compensate the influence of camera environmental temperatures on infrared camera output data.

III. DESIGN OF THERMAL INFRARED DATA COMPENSATION ALGORITHM

Based on the model given by (3), we try to find an algorithm of how to obtain a compensation function \bar{f}_{ij} . To estimate \bar{f}_{ij} , the following optimization problem is solved for each pixel using experimental data

$$\min \|f_{ij}(T_e) - \bar{f}_{ij}(T_e)\| = \min \|y_{ij}(t) - a_{ij}(T_0)x_{ij}(t) - b_{ij}(T_0) - \bar{f}_{ij}(T_e)\| \quad (5)$$

As shown in Fig.2, the function f_{ij} 's have nonlinear characteristics and nonlinear functional approximation is carried out using neural network. In order to find the optimal compensation function for f_{ij} , we consider two

cases. One is a polynomial based functional approximation which optimizes the minimization problem described by (5) with the following two cases for

i) First-order polynomial function

$$\bar{f}_{ij}(T_e) = c_{ij} + d_{ij}(T_e - T_0) \quad (6)$$

ii) Second-order polynomial function

$$\bar{f}_{ij}(T_e) = c_{ij} + d_{ij}(T_e - T_0) + e_{ij}(T_e - T_0)^2 \quad (7)$$

Secondly, we consider a neural network based algorithm for the estimation of the compensation function \bar{f}_{ij} . The neural network for each \bar{f}_{ij} consists of one input, one hidden, and one output layer. Generally, the structure of the neural network we consider is represented by the following input-output equations in each layer.

-Input Layer

$$Y_i^I = W_i^I T_e + B_i^I$$

$$O_i^I = \text{sigmoid}(Y_i^I), i = 1, \dots, N_I \quad (8)$$

-Hidden Layer

$$Y_i^H = \sum_{j=1}^{N_I} W_{ij}^H O_j^I + B_i^H$$

$$O_i^H = \text{sigmoid}(Y_i^H), i = 1, \dots, N_H \quad (9)$$

-Output Layer

$$\bar{f}_{ij}(T_e) = \sum_{j=1}^{N_H} W_j^O O_j^H + B_j^O \quad (10)$$

In (6), N_I, W_i^I, B_i^I , and O_i^I are respectively the number of neurons in the input layer, the weight and offset parameter between i-th neuron and input environmental temperature T_e , and the sigmoid output of i-th neuron in the input layer.

In (9), N_H, W_{ij}^H, B_{ij}^H and O_i^H are respectively the number of neurons in the hidden layer, the weight and offset parameter between i-th neuron in the hidden layer and i-th output O_i^I in the input layer, and the sigmoid output of i-th neuron in the hidden layer. In (9), W_j^O, B_j^O is respectively the weight and offset parameter between j-th neuron in the hidden layer and the sigmoid output in the output layer which is the estimation of the compensation function, \bar{f}_{ij} .

In next section, the performance of the suggested compensation algorithm is investigated for the compensation functions \bar{f}_{ij} .

IV. NUMERICAL PERFORMANCE ANALYSIS

In this section, numerical performance of the suggested simple compensation algorithm (8) is analyzed. As mentioned In this section, numerical performances of compensation algorithms described by (4), (5), and (6)-(8) are analyzed. Here in the experiment, thermal infrared data have been collected using 640x480 Jenoptik infrared cameras. In the experiment black body source was set to be. In the performance comparison, we chose the center pixel, but it does not matter that any pixel is chosen. The results are similar. As mentioned in the previous section, the nominal coefficients a_{ij}, b_{ij} of the center pixel are obtained from Fig.2 at $T_0 = 25^\circ C$ as follows.

$$a_{ij} = 0.0242, b_{ij} = -98.61$$

First, we consider the first order polynomial approximation case. In (4), we have the following results for the coefficients from Fig.2.

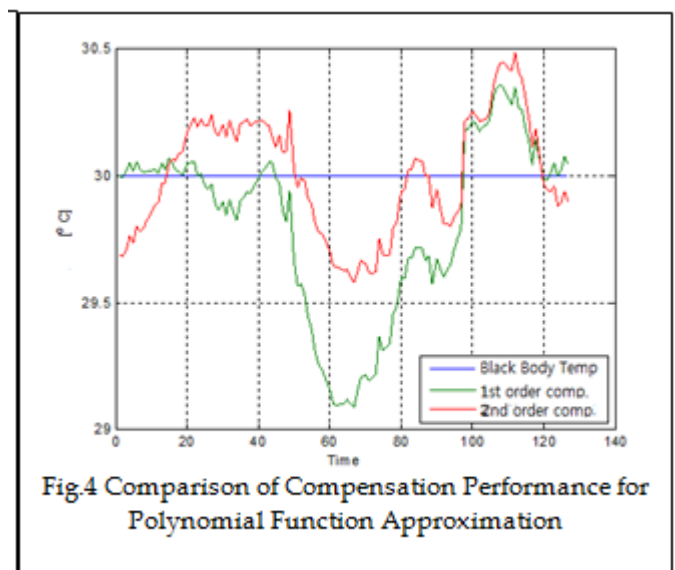
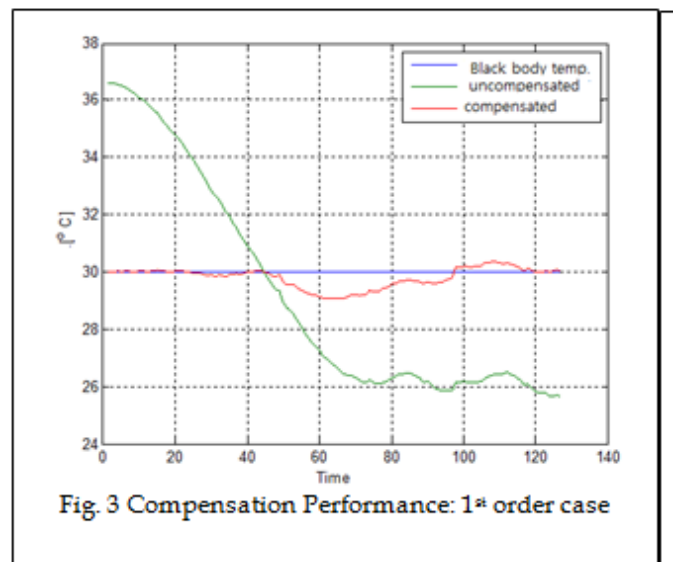
$$c_{ij} = 0, d_{ij} = 0.8333$$

Fig. 3 shows the compensation results. The compensated infrared thermal temperatures are within for the target black body temperature . The temperature accuracy of commercial infrared cameras is usually and for some high price ones.

Next, we consider the second order approximation case. As same in the previous case, using (4), (5), and (8) with (9) and (10), we have the following optimal values for the coefficients

$$c_{ij} = -0.0878, d_{ij} = 0.6115, e_{ij} = 0.0206$$

Fig. 4 shows the comparison results between 1st order compensation and 2nd order compensation. In case of 2nd order compensation, the temperature measurement accuracy is improved to be within $\pm 0.5^\circ C$. This is because the characteristics of the relationship between infrared camera data and camera environmental temperature show nonlinear



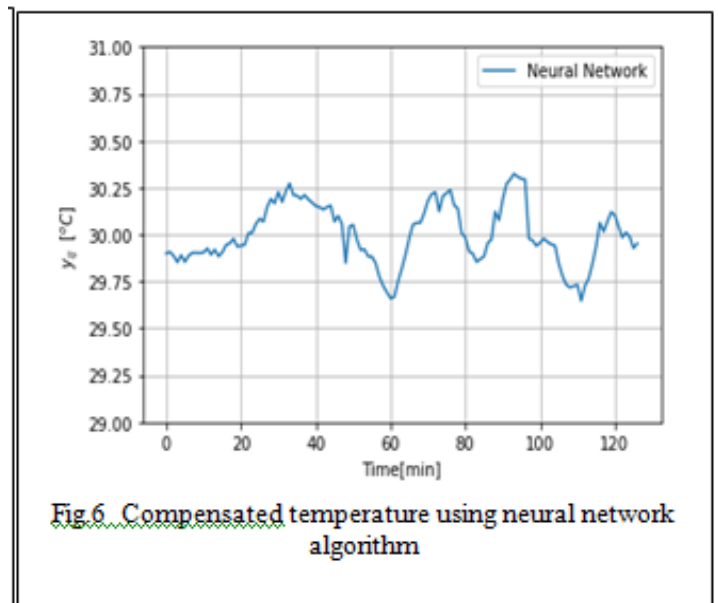
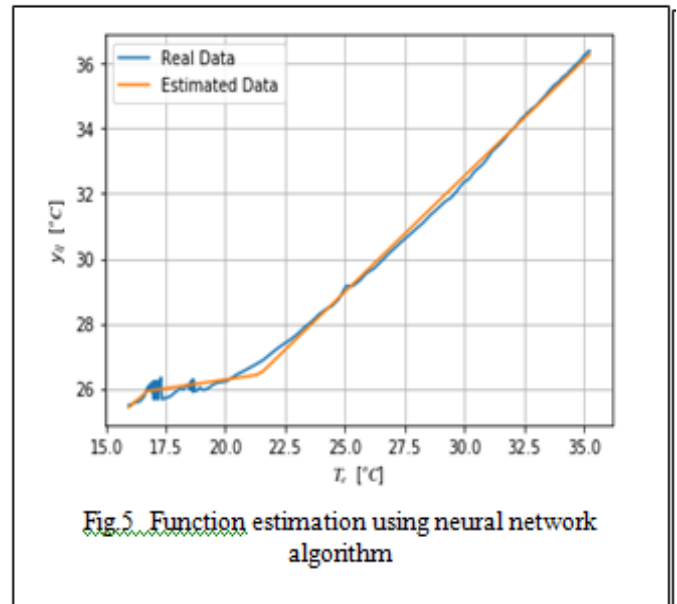
one in Fig. 2. If we choose the estimation of the compensation functions by considering full nonlinearity, the performance will be much more improved than 2nd order polynomial approximation. To see this, the performance a neural network based approach is

investigated for this kind of nonlinear functional approximation. In the neural network described by (6)-(8), we chose the number of neurons in input and hidden layers as follows

$$N_I = 20, N_H = 20$$

The number of neurons in each layer is important. If we choose too small, the estimation performance is not good. If we choose the number of neurons large, then the estimation performance shows very good but the computation takes much time to estimate the compensation values for each neuron. It makes the real time implementation impossible. Now the progress in the technology of GPU makes the real time implementation more easier and possible. By the way, it is not always good that the large number of neurons is chosen in each layer. In some cases, it takes long to train data and it is more easier to make neural networks being in local minima. So it is very important to choose the number of neurons in each layer appropriately. In this example, the nonlinearity of the function which is required to be compensated is not severe. So we just chose it a little bit of small number, 20.

Fig. 5 shows the estimation results of the suggested neural network and Fig. 6 shows the compensation performance of the neural network. As shown in Fig. 5, the nonlinearity is well estimated by the neural network. In order to get the parameters of the neural network, it was trained 10 thousand epochs. The compensated thermal infrared temperatures are well maintained within around the target black body temperature, . As expected, the suggested neural network approach showed the better compensation performance for camera environmental temperature variations.



V. CONCLUSION

In this paper, a compensation algorithm for infrared camera data has been suggested considering environmental parameters such as camera ambient temperature. The experimental results show that the proposed neural network approach is more effective than polynomial functional approach. The compensation algorithm is implemented only by using camera environment temperatures rather than detector substrate temperatures and others. .

VI. ACKNOWLEDGMENT

This paper was supported by Hallym University Research Fund, HRF-201902-014.

VII. REFERENCES

1. J. M. Lloyd, Thermal Imaging Systems (PLENUM press), New York, pp. 257-267, 1982.
2. Gerald C. Holst, Testing and Evaluation of infrared imaging systems, SPIE Optical Engineering Press, USA
3. M. Thomas, D. Newman, M. Froli, D. Pritchett, "Nonuniformity correction of cryogenic 5122 emitter arrays: The 5 minute 5% NUC using FIESTA", Proceeding of SPIE – The International Society for Optical Engineering, Vol. 4366, Orlando, 2001
4. KB, Sai Sanjana, and Srikanth DV. "Thermal Analysis of Advanced IC Engine Cylinder." International Journal of Automobile Engineering Research and Development (IAuERD) ISSN (P) (2016): 2277-4785.
5. H. Budzier, and G. Gerlach, Thermal Infrared Sensors, Theory, optimization and practice, Wiley, Hoboken, NJ., USA, Chichester,UK, 2011.
6. A. Tempelhahn, H. Budzier, V. Krause, and G. Gerlach, "Development of a shutterless calibration process for microbolometer based infrared measurement systems," The e-journal of Nondestructive Testing, 20, ISSN 1435-4934, 2015.
7. Aljamali, Nagham Mahmood, and Rasha Neema. "Synthesis, identification and study of expected biological activity for some (Sulfide, Sulfone) compounds." International Journal of Biological Research and Development (IJBRD) 5.1,(2015):15-30
8. K. G. LeSueur, E. Jovanov, and A. Milenkovic, "Look up table based real-time non-uniformity correction of infrared scene projectors," US Army, Developmental Test Command Redstone Technical Test Center, Bldg. 4500 Redstone Arsenal, AL 35898-8052
9. Bhattacharya, S. S., and S. B. Chaudhari. "Study on structural and thermal properties of polypropylenesilicananocomposite filaments." International Journal of Textile and Fashion Technology 5.1 (2015): 15-22.
10. D. L. Perry and E. L. Dereniak, "Linear theory of nonuniformity correction in infrared staring sensors," Opt. Eng. 32, pp. 1853-1859, 1993.
11. Krishnaveni, J., G. Sowmya, and U. Sudhakar. "Thermal Analysis Of Cylinder Head By Using Finite Element Analysis." International Journal of Mechanical Engineering (IJME) ISSN (P) (2014): 2319-2240.
12. R.C. Harris, M.M.Hayat, E.E. Amstrong, and B.Yasuda, "Scene-based nonuniformity correction using video sequences and registrations," Appl. Opt. 39, pp.1241-1250, 2000
13. Djelti, Hamida. "Thermal effect o the DC characteristics in Al_{0.3}Ga_{0.7}N/GaN high electron mobility transistor." International Journal of Semiconductor Science &Technology (IJSST 4.2 (2014).
14. Fengjun Li, "Function Approximation by Neural Networks," Advances in Neural Networks, pp 384-390 , Springer, 2008The class of models that can be estimated using pool estimation, can as
15. Othman, A. A., et al. "Thermal annealing and UV induced effects on the structural and optical properties of capping free ZnSnano particles synthesized by Co-precipitation method." International Journal of General Engineering and Technology, 3, 9 16 (2014).